Mechanics of surface area regulation in cells examined with confined lipid membranes

Margarita Staykova, Douglas P. Holmes, Clarke Read, and Howard A. Stone[1]

Department of Mechanical and Aerospace Engineering, Princeton University, Princeton, NJ 08544

Edited* by Howard C. Berg, Harvard University, Cambridge, MA, and approved April 7, 2011 (received for review February 11, 2011)

Cells are wrapped in inelastic membranes, yet they can sustain large mechanical strains by regulating their area. The area regulation in cells is achieved either by membrane folding or by membrane exo- and endocytosis. These processes involve complex morphological transformations of the cell membrane, i.e., invagination, vesicle fusion, and fission, whose precise mechanisms are still under debate. Here we provide mechanistic insights into the area regulation of cell membranes, based on the previously neglected role of membrane confinement, as well as on the strain-induced membrane tension. Commonly, the membranes of mammalian and plant cells are not isolated, but rather they are adhered to an extracellular matrix, the cytoskeleton, and to other cell membranes. Using a lipid bilayer, coupled to an elastic sheet, we are able to demonstrate that, upon straining, the confined membrane is able to regulate passively its area. In particular, by stretching the elastic support, the bilayer laterally expands without rupture by fusing adhered lipid vesicles; upon compression, lipid tubes grow out of the membrane plane, thus reducing its area. These transformations are reversible, as we show using cycles of expansion and compression, and closely reproduce membrane processes found in cells during area regulation. Moreover, we demonstrate a new mechanism for the formation of lipid tubes in cells, which is driven by the membrane lateral compression and may therefore explain the various membrane tubules observed in shrinking cells.

supported bilayer | giant vesicles | adhesion

Cells change their surface area during physiological processes such as mitosis (1), motility, phagocytosis (2), and because of mechanical stimulation. For example, neuronal or plant cells regulate their volume and surface area in response to osmotic pressure perturbations (3, 4) and the epithelial cells in the urinary tract and lung alveoli undergo cyclic expansion and compression (5, 6). Because the lipid membrane is inelastic and cannot sustain large strains (7) many cells respond to straining by adding or removing membrane area, through the processes of exo- and endocytosis (2–4, 6, 8). The complex morphological transformations of the cell membrane, such as invagination, fusion, and fission, which occur during exo- and endocytosis, are assisted structurally by various proteins and the composition of the lipid matrix (9, 10), and are mechanically regulated by the membrane tension (3, 11). The latter has been confirmed by observations on cells, which qualitatively indicate that tension is involved in the activation of mechano-sensitive channels, facilitates the fusion process between vesicles and the membrane, and can regulate the rates of exo- and endocytosis (5, 11, 12). Despite the significant progress in disentangling the complex cell responses under mechanical stimuli, it remains difficult to identify the processes of major relevance. Moreover, the available studies on area regulation neglect an important characteristic of the cell membrane, i.e., its confinement to extracellular matrix, the cytoskeleton, other cell membranes, or a solid support. The confinement restricts the modes of the membrane deformation and so influences the mechanisms for surface area regulation. For example, endocytosis has been observed in shrinking protoplasts but not in intact plant cells, which are surrounded by a rigid cell wall (13).

We approach the complex problem of the regulation of cell area in vitro by introducing an experimental setup, which couples a lipid bilayer to the strain-controlled deformation of an elastic sheet (Fig. 1*A*). A fluorescently labeled supported bilayer, composed of 1,2-dioleoyl-*sn*-glycero-3-phosphocholine (DOPC) is prepared on a deformable polydimethylsiloxane (PDMS) substrate (14, 15). For details of the preparation procedures, see *Materials and Methods*. We modulate the strain of the substrate (maximal strains on the order of 0.3–0.5), which results in the equibiaxial lateral expansion or compression of the bilayer (Fig. S1). The structural rearrangements of the membrane in response to the imposed area variations are studied with confocal microscopy.

Results and Discussion

Confined Lipid Bilayers Adjust Their In-Plane Area When Strained. We first outline the main qualitative results identified with our experiments on the controlled membrane straining, which consist of an expansion step, followed by compression. In the initial state of an unstrained substrate (Fig. 1*A*), as a consequence of the preparation procedure, the bilayer contains a number of randomly distributed, adhered vesicles (14). Upon expansion, which significantly exceeds the critical rupture strain, we observe that the bilayer preserves its integrity (indicated by the homogeneous fluorescence) but the number of the vesicles decreases (Fig. 1*B*), which suggests their role as a lipid reservoir. Upon compression, the membrane reduces its in-plane area by the expulsion of a multitude of lipid tubes, which have lengths up to 100 μm and diameters up to few microns (Fig. 1*C*). These morphological transformations are discussed in more details below.

The membrane response to straining observed with our experimental system is entirely passive. It is governed mechanically by the applied lateral strain and the membrane proximity to a confining surface. We argue that a similar mechanism is present also in cells. Indeed, our in vitro findings resemble membrane transformations observed in cells during surface area regulation (Fig. 1*D*). The fusion of vesicles with the expanding bilayer is equivalent
to the exocytosis of cytoplasmic vesicles, which is documented in expanding cells (3, 6, 8). The tubes formed by compressing the supported bilayers strikingly resemble the microtubular invaginations of the membrane observed in shrinking neurons, and renal and plant cells, because such invaginations occur at sites of membrane adhesion to a solid substrate or the cell wall (3, 5, 13). Next, we present the quantitative dynamics of bilayer transformations

Author contributions: M.S., D.P.H., and H.A.S. designed research; M.S. and C.R. performed research; M.S., D.P.H., C.R., and H.A.S. analyzed data; and M.S. and H.A.S. wrote the paper.

The authors declare no conflict of interest.

*This Direct Submission article had a prearranged editor.

[1]To whom correspondence should be addressed. E-mail: hastone@princeton.edu.

This article contains supporting information online at www.pnas.org/lookup/suppl/doi:10.1073/pnas.1102358108/-/DCSupplemental.

Fig. 1. Membrane transformations upon lateral stretching and compression. (*A*) Lipid membrane in the initial state, with firmly adhered vesicles (diameters, $a \approx 200$ nm–4 μm). The membrane is supported on a thin circular PDMS sheet (thickness, $h \approx 100$ μm), which seals one end of an air- or water-filled microfluidic channel. Controlled positive or negative pressure (P) applied by a pump attached to the other end, respectively, inflates or deflates the PDMS sheet, which results in the biaxial lateral expansion or compression of the coupled lipid bilayer (indicated below each image). Confocal micrographs of (*B*) the expanded membrane, where the originally adhered vesicles have been absorbed and (*C*), the compressed membrane, where expulsion of lipid tubes has occurred. Scale bar: 50 μm. (*D*) Analogous membrane transformations, observed in osmotically perturbed cells (3, 5, 13).

upon expansion and compression (for procedures, see *Materials and Methods*).

Lateral Expansion of the Lipid Membranes is Achieved by Vesicle Absorption. We observe that the magnitude to which a membrane can be expanded depends on the vesicle area adherent to the membrane (Fig. 2*A*). Without a lipid reservoir, the bilayer can sustain an area expansion ≈0.02 (Fig. 2*B*), which is comparable to the critical rupture dilation of a giant unilamellar vesicle (GUV) (7, 12). In contrast, the supported bilayer analyzed in Fig. 2*A* expands at least ten times above this critical value. We observe that during the expansion the relative vesicle area, A/A_0, adherent to the bilayer decreases linearly with the bilayer expansion, $\Delta A_m/A_{m0}$ (Fig. 2*A*). Throughout the whole area of observation, smaller vesicles disappear first, whereas the larger vesicles initially shrink and then are absorbed. Thus, by continuously adding lipids, the expanding membrane maintains a constant area/molecule, and so maintains a uniform surface tension below the rupture threshold.

The important role of the membrane tension in promoting membrane fusion has been already reported in cells (12, 16, 17). Using our setup, we are able to visualize the details of this process. We add positively charged GUVs that adhere via electrostatic interactions (18) to the planar bilayer, which is fluorescently labeled by the negative 1,2-dipalmitoyl-*sn*-glycero-3-phosphoethanolamine-*N*-(lissamine rhodamine B sulfonyl) (ammonium salt) (Rh-DPPE) (Fig. 2*C, i*). The adhesion state is accompanied by an exchange of lipids between the GUV and the bilayer (indicated by changes in their fluorescence; see Fig. S2), but does not lead to any visible morphological transformations. Only, after a finite expansion of the supporting substrate, which increases the surface tension of both the planar bilayer and the adhered GUV, do we observe a hemi-fusion of their proximal leaflets. The hemi-fusion, detected as regions of lower fluorescence in our experiments (Fig. 2*C, ii*), is a common intermediate step in the fusion process (9). However, contrary to the usual fusion pathway of pore formation within the hemi-fusion region (9, 17, 19), a pore/pores open on an unadhered portion of the GUV membrane. Thus, our observa-

Fig. 2. Vesicle absorption in an expanding lipid membrane. The bilayer was expanded with a relative rate of 0.002/s. (*A*) Dynamics of vesicle absorption, shown as the dependence of the relative projected vesicle area (A/A_0) adhered to the bilayer to the bilayer relative area increase ($\Delta A_m/A_{m0}$). A_m denotes the area of the in-plane membrane, and, A is the out-of-plane lipid area (adhered vesicles); the subscript 0 refers to the beginning of the expansion, and ΔA_m denotes the membrane area increase between two consecutive video frames. Three images *i*, *ii*, and *iii* are shown for progressively larger membrane expansion. (*B*) The rupture of a supported bilayer at a critical strain of 0.02 (dotted line) in the absence of a vesicle reservoir. Black zones indicate rupture locations. (*C*) The absorption of a GUV (green-yellow) to the expanding planar bilayer (red) shows stages of (*i*) adhesion, (*ii*) hemi-fusion zone and expulsion of the GUV content, and (*iii, iv*) incorporation and diffusion of the vesicle lipids into the bilayer. Scale bars: 20 μm.

tions support an alternative fusion pathway, which has been already suggested by molecular simulations (20, 21). The vesicle expels its contents through the pores (Fig. 2*C*, *ii*) and forms a flat membrane patch on the supported bilayer, in a process reminiscent of vesicle rupture on solid substrates (22). Further expansion leads to the gradual absorption of the flat patch into the lower bilayer, progressing from the outer rim to the center (Fig. 2*C*, *iii* and *iv*). The absorption of even larger GUVs may exhibit some variations, including multiple hemi-fusion zones (Fig. S2).

Lateral Compression of Confined Lipid Membranes Results in Formation of Lipid Tubes. To investigate the mechanics of membrane compression we use lipid bilayers, which are left to equilibrate for a few minutes after expansion. In parallel to the compression of the substrate, we observe that the bilayer reduces its surface area through the expulsion of lipid tubes, whose free ends project into the solution. The nucleation of these tubes is observed after a finite relative area compression (Fig. 3*A*), which varies from experiment to experiment, and is typically 0.02–0.1 (Fig. 3*B* and Fig. S3). The release of lipid area with compression is achieved through the elongation of the tubes and proceeds linearly (Fig. 3*A*). Examination of single tubes (Fig. 3*C*) reveals that (*i*) they are nucleated in a narrow range of compressive strains, and (*ii*) their length increases linearly with compression, with elongation rates 0.1–0.3 μm/s (Fig. S4*A*), which results in a maximum length of about 30 μm; in other experiments, equivalent compression leads to fewer but much longer tubes (Fig. S5). Upon cessation of the compression, the tubes retract during a few hours (Fig. 3*D*), which is significantly longer than the relaxation of tethers extracted from GUVs (23).

To interpret our observations we note that the compressive strain of the substrate translates into in-plane compression of the supported lipid bilayer (no area relaxation occurs through bending), which decreases the area per lipid molecule, and thus the effective tension of the bilayer. At a critical tension, the bilayer destabilizes and expels lipid tubes to relax its area in the plane. A similar type of collapse has been theoretically explained for free-standing lipid monolayers (24) and bilayers (25, 26), and transiently observed on GUVs upon a rapid lipid exchange (27). A difference between prior theory and our experiments arises due to the confinement of our bilayers for which destabilization is influenced by interactions with the substrate. For example, the experimentally observed dynamics of tube expulsion, i.e., the discrete sites and the different compressive thresholds of tube nucleation, as well as the varying elongation rates, suggest, respectively, local variations in the bilayer adhesion energy, surface tension, and shear viscosity, which arise presumably from the nonhomogenous interactions with the substrate. Similar heterogeneities are expected to occur in cells. We have not been able to study the structure of the tubes with submicroscopic resolution, but recent research suggests that they are hollow cylinders enclosed by a bilayer wall (28). The elongation of the lipid tubes with further compression may be rationalized by a Marangoni flow, as observed in lipid tethers connecting vesicles of different tension (29, 30). The apparent stability of the tubes may be explained by the higher shear modulus of the supported bilayer, which slows the membrane bending kinetics, and the equilibrated tension at the cessation of the compression. Finally, we note that lipid tubes were previously shown to form in vivo in cells by molecular motors exerting point forces (31) or by the curving of the membrane through molecular (32) and chemical interactions (33). Our observations indicate a unique passive route for tube formations, determined solely by mechanical constraints on the membrane.

Lipid Bilayers Reversibly Adjust Their Area. Cells must reversibly change their surface area during cycles of stress. To probe the reversibility of the induced membrane transformations we use cycles of mechanical expansion and compression. The response of a bilayer, with tubes formed upon a previous compression, to a new cycle of expansion is shown in Fig. 4. By measuring the projected area of the tubes as a function of the membrane expan-

Fig. 3. Tube formation upon membrane compression. (*A*) Dynamics of tube expulsion, shown as the dependence of the relative projected tube area (A/A_f) to the relative membrane area compression, $\Delta A_m/A_{m0}$. The subscript f refers to the end of the compression and ΔA_m denotes the membrane area decrease between two consecutive video frames. Confocal micrographs of the tubes in the initial (*i*), intermediate (*ii*), and final (*iii*) stages of the compression are provided. Scale bar: 10 μm. (*B*) Critical compressive strain for tube nucleation, as determined from many experiments. (*C*) The relative increase of the tube length, L (micrometers) as a function of $\Delta A_m/A_{m0}$ is shown for three tubes. A schematic of our interpretation of the mechanism underlying the tube formation are depicted in *i*, *ii*, and *iii*. (*D*) Tube retraction time at the cessation of the compression.

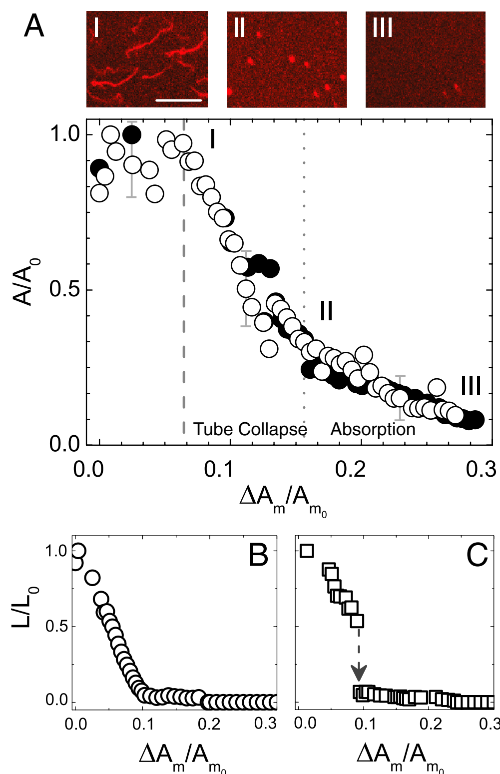

Fig. 4. Tube retraction in an expanding lipid bilayer. (*A*) Projected relative area of the tubes and later of the spherical formations (A/A_0) versus the relative membrane area expansion $\Delta A_m/A_{m0}$, as measured on the same bilayer sample for different expansion cycles (open and closed circles). Confocal micrographs are provided of (*i*) the beginning and (*ii*) the end of the tube collapse phase, and (*iii*) the consequent stage of aggregate absorption. Scale bar: 20 μm. Decrease of the tube length (L/L_0) as a function of $\Delta A_m/A_{m0}$ depicts two different dynamics: gradual tube shortening into an aggregate (*B*) and tube shortening followed by a rapid collapse into an aggregate (*C*).

sion, $\Delta A_m/A_{m0}$, and comparing with the optical images, we distinguish two regimes in the dynamics of the tube absorption. After a finite relative expansion $\Delta A_m/A_{m0}$, there is a rapid decrease in the projected tube area, which reflects the simultaneous retraction of the tubes into spherical shapes (Fig. 4*A, i* and *ii*). This process occurs about 150 times faster than the passive tube relaxation (Fig. S4*B*), but is slower than retraction of lipid tethers in GUVs (23). The retraction may follow two pathways: a gradual retraction (Fig. 4*B*) or a snap-like transition into spherical formations (Fig. 4*C*). The retraction phase is followed by a slower phase of gradual absorption of the spherical lipid formations into the expanding bilayer. Because of insufficient microscopic resolution, we are unable to say whether these formations are vesicles or lipid aggregates but we note that similar lipid aggregates have been observed by transmission electron microscopy in shrinking plant guard cells (13). Finally, we observe that during cyclic expansion and compression, tubes form and retract recurrently at the same location on the bilayer. This result is consistent with observations on cells (3, 5) and can be explained by the discrete adhesion of the cell membrane to the confining surfaces.

In summary, our in vitro findings imply that changes in the surface tension upon lateral straining directly trigger compensatory remodeling of lipid membranes, which depends solely on the physical properties of the lipid matrix and the effects of the membrane confinement. The generality of our findings and their similarity to observations on real cells suggest that similar mechanisms may also be employed by cells for surface area regulation. Moreover, our observation that lipid tubes form mechanically from confined and laterally compressed membranes indicate a unique passive pathway for their formation. As already suggested in the literature, such a mechanism may play an important role for preserving the adhesion contacts of cells during area variations (34). Moreover, the mechanism is also expected to be applicable to membranes laterally compressed by rapid intake of lipids or proteins (27, 28).

Our future research will address the details of the membrane confinement (e.g., adhesion strength, discretization of adhesion contacts) and the influence of the strain rate and the bilayer composition on membrane remodeling upon expansion and compression. We are also interested in the cooperativity of the structural rearrangements of expanding or compressing membranes, for example the mutual interactions between tubes and their conformational response to, for example, curvature-sensitive molecules.

Materials and Methods

Chemicals. DOPC, 1,2-dioleoyl-3-trimethylammonium-propane (chloride salt) (DOTAP), Rh-DPPE, 1,2-dioleoyl -*sn*-glycero-3-phosphoethanolamine-*N*-(lissamine rhodamine B sulfonyl) (ammonium salt) (Rh-DOPE), and 1-oleoyl-2-[12-[(7-nitro-2-1,3-benzoxadiazol-4-yl)amino]lauroyl]-*sn*-Glycero-3-phosphocholine (NBD-PC) were all purchased from Avanti Polar Lipids. Chloroform, trizma hydrichloride (Tris·HCl), and sucrose were purchased from Sigma Aldrich.

Materials. For the experimental setup we use PDMS and curing agent from Dow Corning (Sylgard 184 Silicone Elastomer Kit, catalog no. 240 401 9862), microscope slides from Fisher Scientific (catalog no 12-544-1), and cover glasses from VWR (catalog no. 48366 045). For the preparation procedure of GUVs we used Indium Tin Oxide coated glasses (ITO glasses) from Delta Technologies (no. X180).

Supported Lipid Bilayer. Supported bilayers are prepared using standard vesicle fusion technique (15, 35, 36). A thin film of 1 mg lipids (DOPC and Rh-DPPE in a 99.5/0.5 mol % ratio) is dried overnight under vacuum on the walls of a glass vial. The dried lipid film is rehydrated in a Tris·HCl buffer (10 mM Tris·HCl, 150 mM NaCl, 2 mM CaCl2, adjusted with 1 M HCl to pH ≈ 7.5) to a concentration of 0.5 mg lipids/mL, resulting in the formation of a turbid suspension, which is then sonicated using a probe sonicator (Branson) for 10 min at 40% power to obtain small unilamellar vesicles (SUV). A dilution of the SUVs suspension with Tris·HCl buffer at a 20∶1 volume ratio is spread over the clean hydrophilic PDMS surface (see below), in a volume created by a 1 × 1 × 0.5 cm gasket. Incubation for about 30–60 min results in the formation of a supported lipid bilayer. The excess of unfused vesicles is removed by washing with ultrapure water. For the microscopic recordings the whole volume is then sealed with a coverslip. In the absence of large defects, fluorescently labeled DOPC bilayers on PDMS planar substrates are known to be homogenous (15), except for some vesicles adhered onto the bilayer (14). The number of vesicles depends on the buffer composition, the incubation time, the extent of washing, etc. To prove that the choice of the fluorescent marker does not influence the results, we perform also experiments with SUVs, labeled by Rh-DOPE or NBD-PC.

Experimental Setup. PDMS (with 10 wt % curing agent) stamps of a straight microfluidic channel are manufactured by the soft lithography technique (37). On the PDMS stamp, we punch two holes of 1 mm in diameter with a biopsy puncher (Miltex) at both ends of the channel and plasma-seal it to a microscope slide to close the channel. The inlet hole is connected via a polyethylene tube to a syringe. Over the second hole, we bond a 100 μm thick PDMS sheet (obtained by spin-coating PDMS), whose surface above the channel will serve as a support for the lipid bilayer. Note that the microfluidic channel is used only to apply pressure on the PDMS sheet; therefore, its dimensions are not of major importance. The PDMS surface is cleaned via sonication for 10 min in ethanol, followed by water, and its surface is converted to hydrophilic via exposure to plasma for 10 s in a Harrick Plasma Cleaner/Sterilizer PDC-32G at maximum power, shortly before introducing the lipids.

Stretching and Compressing Lipid Membranes. It has been shown that lipid bilayers strongly couple to PDMS surfaces (15). Therefore, to induce lateral expansion or compression of the bilayer, we simply expand or compress the area of the PDMS sheet underneath by applying pressure via a microsyringe

pump (Harvard Apparatus). A positive pressure underneath the PDMS sheet will inflate it, which leads to equibiaxial stretching of its surface area. A consequent deflation of the PDMS balloon will lead to a surface area compression. The rates of increasing/decreasing the pressure in the channel, as controlled via the syringe pump, and the consequent rates of inflation/deflation of the PDMS sheet, are linearly proportional to the rate of surface area change of the PDMS sheet, but only for small area variations. Above approximately 25% area variation from the flat initial state, the area of the PDMS sheet changes more rapidly (Fig. S1*A*), which is in agreement with the nonlinearity associated with inflating/deflating a thin-walled shell (38). Therefore, controlled rate experiments are possible by properly calibrating the PDMS expansion.

Preparation of GUVs. GUVs are prepared from DOPC, DOTAP, and the fluorescent lipid NBD-PC in 94/3/3 mol percent, using the electro-formation method (39). A small amount of the 4 mM lipid mixture in chloroform is dried over the conductive surface of two indium tin oxide (ITO) glass slides. A chamber constructed from these ITO surfaces, and separated by a 2 mm-thick Teflon gasket, is filled with 0.1 M sucrose solution and subjected to an alternating current (900 mV, 10 Hz frequency). After about 4 h, we obtain GUVS with an average size of 20 μm. A small amount of the GUV suspension is introduced to the chamber containing the supported bilayer in Tris·HCl buffer (at room temperature). The denser and positively charged vesicles (containing DOTAP) sediment and adhere by electrostatic forces on the slightly negatively charged supported bilayer (containing Rh-DPPE).

Image Analysis. The membrane transformations during PDMS expansion and compression are recorded by an inverted confocal laser scanning microscope (Leica Microsystems), in a time sequence of confocal micrographs (one frame per 1.3 s). For the analysis, we define on the first image a small rectangular area on the supported bilayer, where at least four vesicles are unabsorbed, and follow the change in the area for every image in the sequence. The selected area must be around the center of the circular PDMS sheet to ensure that it is under an equibiaxial strain. We use a homemade MATLAB code to estimate the two-dimensional projected area of the vesicles/tubes onto the selection area of the bilayer. Because the tubes and the adhered vesicles appear brighter than the bilayer in the plane, we simply count the pixels with an intensity above a certain threshold for every frame taken during the membrane expansion and compression. Next, we obtain the relative projected areas, by dividing the current area by the initial (for expansion) or the final (for compression) projected area. The lipid tubes assume random configurations in space, which constantly vary in time. Therefore, the measure of the relative projected area reflects dynamics of the changes in the area during vesicle absorption and tube expulsion. We use ImageJ to estimate the projected length of the tubes by manually tracing them.

ACKNOWLEDGMENTS. We thank S. Lecuyer and P. Kim for help with experiments and P. Nassoy and L. Staykov for helpful feedback. We thank Princeton University and the Project X Fund for financial support.

1. Boucrot E, Kirchhausen T (2007) Endosomal recycling controls plasma membrane area during mitosis. *Proc Natl Acad Sci USA* 104:7939–7944.
2. Kay RR, Langridge P, Traynor D, Hoeller O (2008) Surface area regulation: Underexplored yet crucial in cell motility. *Nat Rev Mol Cell Biol* 9:662 (lett).
3. Morris E, Homann U (2001) Cell surface area regulation and membrane tension. *J Membr Biol* 179(2):79–102.
4. Shope JC, DeWald DB, Mott KA (2003) Changes in surface area of intact guard cells are correlated with membrane internalization. *Plant Physiol* 133:1314–1321.
5. Apodaca G (2002) Modulation of membrane traffic by mechanical stimuli. *Am J Physiol Renal Physiol* 282:179–190.
6. Fisher J, Levitan I, Margulies S (2004) Plasma membrane surface increases with tonic stretch of alveolar epithelial cells. *Am J Respir Cell Mol Biol* 31:200–208.
7. Evans E, Hochmuth R-M (1978) *Topics in Membrane and Transport*, eds A Kleinzeller and FEC Bronner (Academic, New York), Vol 10, pp 1–64.
8. Groulx N, Boudreault F, Orlov S, Grygorczyk R (2006) Membrane reserves and hypotonic cell swelling. *J Membr Biol* 214(1):43–56.
9. Chernomordik L, Kozlov M (2008) Mechanics of membrane fusion. *Nat Struct Mol Biol* 15:675–683.
10. Lenz M, Morlot S, Roux A (2009) Mechanical requirements for membrane fission: Common facts from various examples. *FEBS Lett* 583:3839–3846.
11. Dai J, Sheetz M (1995) Regulation of endocytosis, exocytosis, and shape by membrane tension. *Cold Spring Harbor Symp Quant Biol* 60:567–571.
12. Hamill O, Martinac B (2001) Molecular basis of mechanotransduction in living cells. *Physiol Rev* 81:685–740.
13. Li B, et al. (2010) Excretion and folding of plasmalemma function to accommodate alterations in guard cell volume during stomatal closure in Vicia faba L. *J Exp Bot* 61:3749–3758.
14. Nollert P, Kiefer H, Jähnig F (1995) Lipid vesicle adsorption versus formation of planar bilayers on solid-surfaces. *Biophys J* 69:1447–1455.
15. Sanii B, Smith A, Butti R, Brozell A, Parikh A (2008) Bending membranes on demand: Fluid phospholipid bilayers on topographically deformable substrates. *Nano Lett* 8:866–871.
16. Finkelstein A, Zimmerberg J, Cohen FS (1986) Osmotic swelling of vesicles—its role in the fusion of vesicles with planar phospholipid-bilayer membranes and its possible role in the exocytosis. *Annu Rev Physiol* 48:163–174.
17. Grafmüller A, Shillcock J, Lipowsky R (2007) Pathway of membrane fusion with two tension-dependent energy barriers. *Phys Rev Lett* 98:218101.
18. Solon J, Streicher P, Richter R, Brochard-Wyart F, Bassereau P (2006) Vesicles surfing on a lipid bilayer: Self-induced haptotactic motion. *Proc Natl Acad Sci USA* 103:12382–12387.
19. Haluska C, et al. (2006) Timescales of membrane fusion revealed by direct imaging of vesicle fusion with high temporal resolution. *Proc Natl Acad Sci USA* 103:15841–15846.
20. Müller M, Katsov K, Schick M (2003) A new mechanism of model membrane fusion determined from Monte Carlo simulations. *Biophys J* 85:1611–1623.
21. Smeijers AF, Markvoort AJ, Pieterse K, Hilbers PAJ (2006) A detailed look at vesicle fusion. *J Phys Chem B* 110:13212–13219.
22. Lenz P, Johnson JM, Chan Y-HM, Boxer SG (2006) Tension-induced pore formation and leakage in adhering vesicles. *Europhys Lett* 75:659–665.
23. Rossier O, et al. (2003) Giant vesicles under flows: Extrusion and retraction of tubes. *Langmuir* 19:575–584.
24. Baoukina S, Monticelli L, Jelger-Risselada H, Marrink SJ, Tieleman DP (2008) The molecular mechanism of lipid monolayer collapse. *Proc Natl Acad Sci USA* 105:10803–10808.
25. Rao M, Sarasij R (2001) Active fusion and fission processes on a fluid membrane. *Phys Rev Lett* 87:128101.
26. Girard P, Juelicher F, Prost J (2004) Fluid membranes exchanging material with external reservoirs. *Eur Phys J E Soft Matter Biol Phys* 14:387–394.
27. Solon J, et al. (2006) Negative tension induced by lipid uptake. *Phys Rev Lett* 97:098103.
28. Domanov YA, Kinnunen PK (2006) Antimicrobialpeptides Temporins B and L induce formation of tubular lipid protrusions from supported phospholipid bilayers. *Biophys J* 91:4427–4439.
29. Karlsson R, et al. (2002) Moving-wall-driven flows in nanofluidic systems. *Langmuir* 18:4186–4190.
30. Dommersnes P, Orwar O, Brochard-Wyart F, Joanny J (2005) Marangoni transport in lipid nanotubes. *Europhys Lett* 70:271–277.
31. Roux A, et al. (2002) A minimal system allowing tubulation with molecular motors pulling on giant liposomes. *Proc Natl Acad Sci USA* 99:5394–5399.
32. Stachowiak JC, Hayden CC, Sasaki DY (2010) Steric confinement of proteins on lipid membranes can drive curvature and tubulation. *Proc Natl Acad Sci USA* 107:7781–7786.
33. Fournier JB, Khalifat N, Puff N, Angelova MI (2009) Chemically triggered ejection of membrane tubules controlled by intermonolayer friction. *Phys Rev Lett* 102:018102.
34. Morris CE (2001) Mechanosensitive membrane traffic and an optimal strategy for volume and surface area regulation in CNS neurons. *Am Zool* 41:721–727.
35. Hovis JS, Boxer SG (2001) Patterning and composition arrays of supported lipid bilayers by microcontact printing. *Langmuir* 17:3400–3405.
36. Subramaniam A, Lecuyer S, Ramamurthi K, Losick R, Stone HA (2010) Particle/fluid interface replication as a means of producing topographically patterned polydimethylsiloxane surfaces for deposition of lipid bilayers. *Adv Mater* 22:2142–2147.
37. Duffy DC, McDonald JC, Shueller OJA, Whitesides GM (1998) Rapid prototyping of microfluidic systems in poly(dimethylsiloxane). *Anal Chem* 70:4974–4984.
38. Gent AH (2005) Elastic instabilities in rubber. *Int J Non Linear Mech* 40:165–175.
39. Angelova M, Dimitrov DS (1986) Liposome electroformation. *Faraday Discuss* 81:303–311.